

LETTER TO EDITOR

Overexpression of miR-483-5p is confined to metastases and linked to high circulating levels in patients with metastatic pheochromocytoma/paraganglioma

Dear Editor,

Pheochromocytomas/paragangliomas (PPGL) are tumors of the adrenal medulla and paraganglia. Currently, there is no means to distinguish metastatic from non-metastatic PPGL based on histopathological criteria. Consequently, patients at risk of progression require a long-term follow-up. Here, by conducting complementary analyses of large collections of primary tumors, metastatic tissues, and liquid biopsies, we uncovered that miR-483-5p is overexpressed in metastatic tissues compared to primary tumors, whereas the highest levels were detected in the serum of metastatic patients. Further integrative genomic analyses suggest that miR-483-5p might be involved in metastasis-related regulatory networks. These findings pinpoint circulating miR-483-5p levels as a promising noninvasive biomarker for the presence of metastasis, which could be useful for guiding patient surveillance.

Although large tumor size, extra-adrenal location, and germline Succinate Dehydrogenase Complex, Subunit B (*SDHB*) mutations are established risk factors for metastatic PPGL (mPPGL), there is a lack of tumor molecular biomarkers.¹ In a recent study, we identified a six-miRNA prognostic signature (miR-21-3p, miR-183-5p, miR-96-5p, miR-182-5p, miR-551b-3p, and miR-202-5p) in primary tumors, and we detected high levels of four of these miRNAs in the circulation of metastatic patients.² To extend the analysis of informative miRNAs, here we evaluated miR-483-5p and miR-210-3p that have been suggested as biomarkers of mPPGL³⁻⁶ and many other tumor types. To this end, the expression of these two miRNAs was interrogated in the largest series of miRNome tumor data ($n = 443$, $n = 7$ metastases) published so far (as detailed elsewhere²), and validated by Quantitative Reverse Transcription PCR (RT-qPCR) in an independent series of tumor tissues ($n = 107$, $n = 24$ metastases) (Table S1). Circulating levels were assessed in serum from 26 patients and 10 healthy controls using TaqMan assays and droplet digital

polymerase chain reaction (PCR). Additional integrative miRNA-483-5p-transcriptome analyses were performed to identify gene sets enriched upon miRNA deregulation and its potential targets.

The expression of miR-210-3p was higher in metastatic than in non-metastatic primary tumors in the published series. However, this result was not reproduced in the validation series (Figure S1) nor in the circulation of metastatic patients, indicating that miR-210-3p is not informative for discriminating metastatic from non-metastatic PPGL. Regarding miR-483-5p, we found that its expression did not exhibit significant differences between non-metastatic and metastatic primary tumors (Figure 1A). However, significant overexpression of miR-483-5p was readily detected in metastatic tissues compared to primary tumors in both, published ($P = 2.0 \times 10^{-3}$) and validation series ($P = 2.0 \times 10^{-5}$) (Figure 1A). High expression levels of miR-483-5p in metastatic tissues were confirmed in a separated analysis of 17 paired primary-metastases ($P = 6.5 \times 10^{-4}$; Figure 1B). To our knowledge, this is the first time a potential biomarker of mPPGL is evaluated in a large series of metastatic tissues.

Assessment of circulating miR-483-5p in the series of liquid biopsies revealed higher levels in metastatic than in non-metastatic patients ($P = .002$) (Figure 1A). Accordingly, paired samples from patients with single PPGL for whom blood was collected before surgery, did not show significant correlations of circulating miR-483-5p with primary tumor sizes ($n = 16$; $r = 0.142$, $P = .599$) nor with its expression in primary tumors ($n = 9$; $r = -0.237$, $P = 0.54$). Circulating miR-483-5p was the finest marker to indicate the presence of metastases (OR = 6.4, 95% CI = 1.12-36.44, $P = .036$) and the only one selected after applying a stepwise conditional logistic regression to define the best classifier compared to circulating levels of miRNAs with prognostic value when assessed in primary tumors² (Figure 1C). Further receiver operating characteristic

This is an open access article under the terms of the [Creative Commons Attribution](https://creativecommons.org/licenses/by/4.0/) License, which permits use, distribution and reproduction in any medium, provided the original work is properly cited.

© 2020 The Authors. *Clinical and Translational Medicine* published by John Wiley & Sons Australia, Ltd on behalf of Shanghai Institute of Clinical Bioinformatics

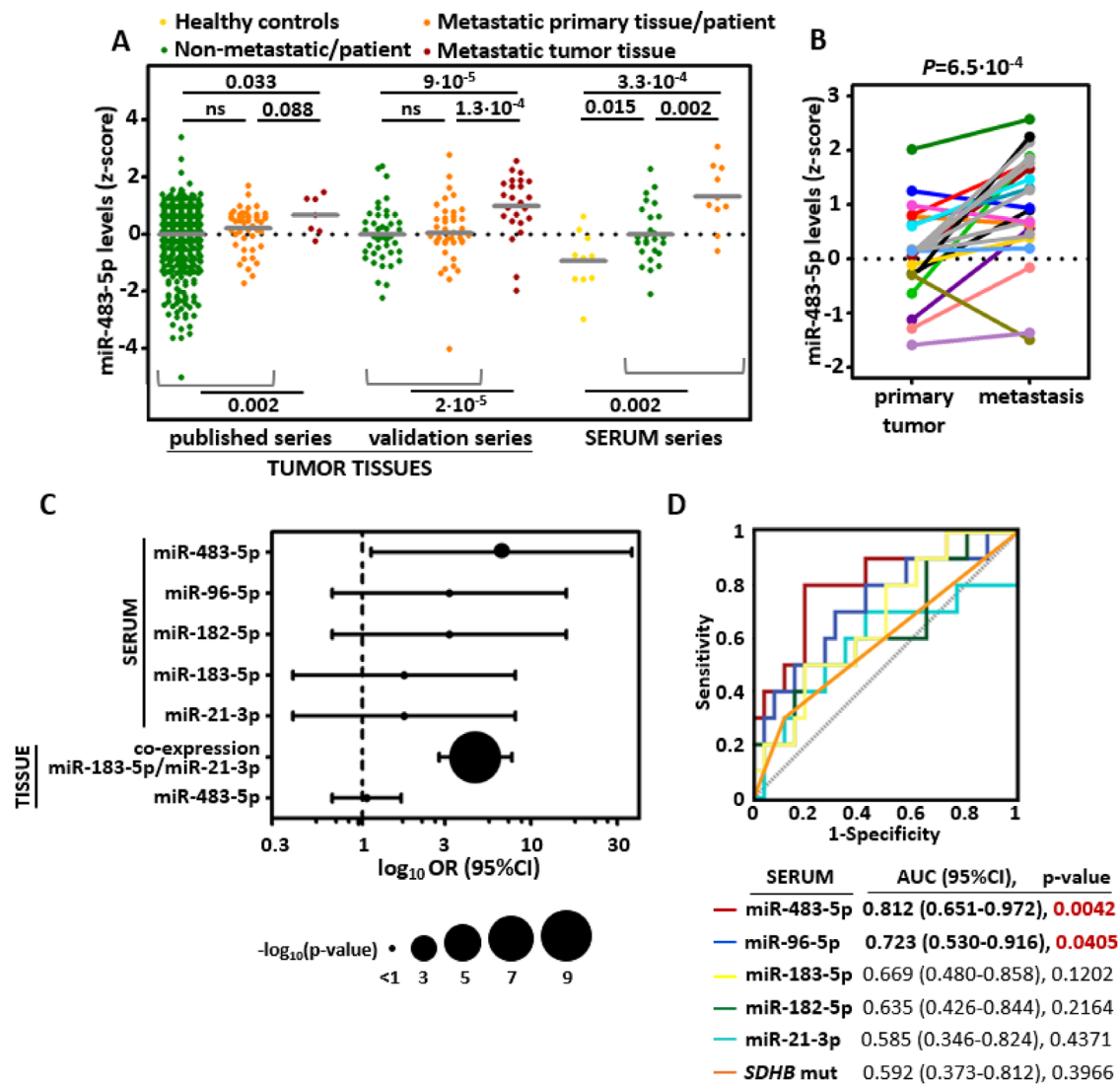


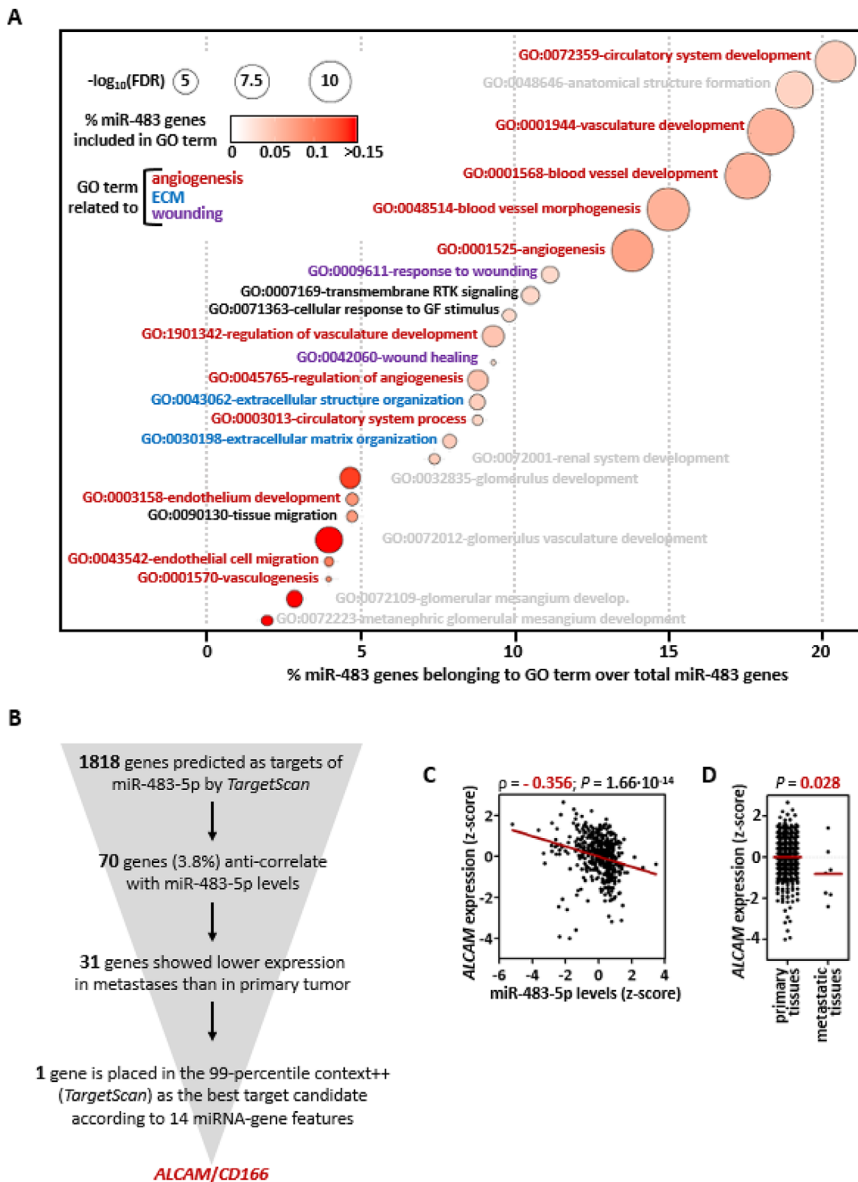
FIGURE 1 High levels of miR-483-5p are detected in metastases and serum from mPPGL patients. **A**, Log₂ normalized expression from the different series is displayed as a transformed z-score (centered to the mean of non-metastatic group per each series). Differences in the expression levels in each series were tested by a one-sided nonparametric Mann-Whitney test. The mean is shown per each group. **B**, Related to (A), miR-483-5p levels in paired primary tumor-metastatic tissues (n = 17). Each dot represents the level of miRNA in tumor tissue; each color belongs to a different patient. One-tailed paired *t*-test was applied to test for differences between paired samples. **C and D**, Comparison of circulating levels of miR-483-5p and previously reported miRNAs in mPPGL. Except for miR-483-5p, these data were extracted from reported experiments.² **C**, Forest plot showing the odds ratio (OR) obtained from a binary logistic regression applied to test for associations between serum levels of miRNAs and the presence of metastasis in PPGL patients. Also, OR related to risk of metastasis and miRNA expression in tissue is shown for the previously reported classifier (miR-183-5p/miR-21-3p) (extracted from Calsina et al) and for miR-483-5p. The level of each miRNA was expressed as a dichotomous variable using the median level of each miRNA as the cutoff for analyses. Error bars represent the 95% confidence interval (CI), and the diameter of the bubbles is proportional to $-\log_{10}(P\text{-value})$. For miR-183-5p/miR-21-3p classifier, the high expression (above median) of both miRNAs at the same time was considered as the cutoff. **D**, Receiver operating characteristic curve analysis showing the accuracy of the different circulating miRNA to discriminate mPPGLs from no-mPPGL, and *SDHB* status in the serum series

curve (ROC) analysis showed that circulating miR-483-5p has the highest accuracy as presence of metastasis discriminator (Area Under the Curve (AUC) = 0.81, 95% CI = 0.651-0.972, $P = 4.0 \times 10^{-3}$). This accuracy was comparable to the reported for miR-21-3p/miR-183-5p levels in primary tumors (AUC = 0.804, $P = 4.67 \times 10^{-18}$)²

and was largely superior to the *SDHB* status (Figure 1D). Therefore, the miR-483-5p appears as the most promising biomarker of mPPGL when assessed in liquid biopsies. Collectively, these data indicate that miR-483-5p is likely released at sites of metastatic colonization and may account for the high circulating levels detected in

FIGURE 2 Functional enrichment and integrative analyses of miR-483-5p and transcriptome data.

A, Bubble diagram showing the most significant biological processes obtained after applying STRING (<https://string-db.org/>) using the list of genes that correlate significantly with miR-483-5p levels. The color of the bubbles indicates the percentage of genes that correlate with miR-483-5p levels (here designated as miR-483 genes) and are included in each specific Gene Ontology (GO) term. The diameter of the bubbles is proportional to the $-\log_{10}(\text{FDR})$ obtained with STRING tool. The x-axis shows the percentage of miR-483 genes that are present in each GO term over the total number of miR-483 genes. GO terms in red indicate gene sets related to angiogenesis, in blue gene sets related to extracellular matrix (ECM), and in purple gene sets related to wounding. **B**, Workflow and filtering criteria used for analysis of miR-483-5p targets, leading to the identification of *ALCAM*. **C**, Scatter plot showing the correlation between miR-483-5p and *ALCAM* expression from published series ($n = 443$). Levels of miR-483-5p and *ALCAM* are displayed as a transformed z-score (centered at the mean of the expression in each series). Spearman's correlation (ρ) and P values are shown. **D**, *ALCAM* levels in primary tissues and metastases from the published series. Differences in the expression were tested by a one-sided nonparametric Mann-Whitney test. The mean is shown per each group



metastatic patients. From the clinical standpoint, circulating miR-483-5p could be used to inform when indolent patients become metastatic.

Notably, by scaling miR-483-5p expression across 380 metastases from the TCGA consortium, we found that the two metastatic tissues of the PPGL cohort display the highest levels of miR-483-5p (Figure S2). According to the human miRNA tissue atlas, the expression of miR-483-5p is not tissue specific. Thus, overexpression of this miRNA might play active roles in PPGL cells at the metastatic niche. To explore this possibility, we carried out a comprehensive omics data integration.

Correlation analysis of miR-483-5p and gene expression data revealed 152 genes associated with miR-483-5p levels ($-0.4 > \rho > 0.4$ and $P \leq 1 \cdot 10^{-4}$). Functional enrichment analysis suggested miR-483-5p as an important regulator of angiogenesis, wound healing, and extracellular

matrix organization (Figure 2A), which are tightly related to invasion/metastasis. This finding is in line with the fact that miR-483-5p regulates the expression of its host gene *IGF2*, a stimulator of angiogenesis,⁷ and that *IGF2* expression highly correlates with miR-483-5p in PPGL and other cancers³ (Figure S3). The involvement of miR-483-5p in angiogenesis and extracellular matrix regulation has been demonstrated in models of ischemic disease and osteoarthritis,^{8,9} whereas direct regulation of wound healing by miR-483-5p was reported in a model of skin repair.¹⁰

To identify miR-483-5p targets that could better explain its potential oncogenic functions, we followed the workflow described in Figure 2B. A single gene, activated leukocyte cell adhesion molecule (*ALCAM*)/*CD166*, was identified as the best target candidate. *ALCAM* 3' Untranslated Region (UTR) sequence has an 8 mer-seed matched site for miR-483-5p (Figure S4), and its expression levels

significantly anti-correlate with miR-483-5p ($n = 443$, $\rho = -0.356$; $P = 1.66 \times 10^{-14}$; Figure 2C). It has been reported that ALCAM expression decreases with tumor progression,¹¹ which entails a poor prognosis. In this regard, we observed a lower expression in metastatic tissues compared to primary tumors in our PPGL series ($P = .028$; Figure 2C), as well as in the TCGA PANCAN cohort ($n = 396$ metastatic tissues, $n = 9712$ primary tumors; $P = 5.8 \times 10^{-102}$). Since previous reports have demonstrated that miR-483-5p directly binds *ALCAM* and regulates its expression in lung adenocarcinoma,¹² the functional interaction miR-483-5p/*ALCAM* may shed light on the understanding of PPGL metastatic niche and warrants further investigation.

In conclusion, while assessment of miR-183-5p/miR-21-3p in primary tumors improves the stratification of patients at risk of metastasis at the time of diagnosis,² here we suggest circulating miR-483-5p, a miRNA potentially related to metastatic colonization, as a promising noninvasive biomarker for the follow-up of that group of patients. These preliminary results encourage prospective studies aimed at ascertain the clinical relevance of such biomarkers.

ACKNOWLEDGMENTS

This study was funded by European Union Seventh Framework Program (FP7/2007-2013) under grant agreement (grant number: 259735), Horizon 2020 (grant number: 633983), Institut National du Cancer and Direction Générale de l'Offre de Soins (DGOS), Programme de Recherche Translationnelle en cancérologie (PRT-K 2014, COMETE-TACTIC, INCa_DGOS_8663), the Plan Cancer: Appel à projets Epigénétique et Cancer 2013 (EPIG201303 METABEPIC), Agence Nationale de la Recherche (ANR-2011-JCJC-00701 MODEOMAPP), Instituto de Salud Carlos III (ISCIII), Acción Estratégica en Salud, cofounded by FEDER (PI14/00240 and PI17/01796) and the Paradifference Foundation. Bruna Calsina was supported by Rafael del Pino Foundation (Becas de Excelencia Rafael del Pino 2017) and currently by ISCIII project PI17/01796. We thank all members of the Genetics Department, Biological Resources Center and Tumor Bank Platform, Hospital européen Georges Pompidou (BB-0033-00063) for technical support.

CONFLICT OF INTEREST

The authors declare that there is no conflict of interest that could be perceived as prejudicing the impartiality of the research reported.

ETHICS APPROVAL AND CONSENT TO PARTICIPATE

This study was conducted ethically in accordance with the Declaration of Helsinki. Tumors from the validation

series were collected, thanks to the CNIO Tumor bank with the approval of the institutional review board, and the Bioethics and animal welfare committee of the Carlos III Health Institute. For analysis of liquid biopsies, all patients signed a written consent for the genetic study of the blood and/or tissue samples. This study was approved by the institutional review board (Comité de Protection des Personnes [CPP] Ile de France III, June 2012).


AUTHOR CONTRIBUTIONS

Conception and supervision: Castro-Vega and Gimenez-Roqueplo. Design of the study: Castro-Vega, Calsina, Robledo, and Gimenez-Roqueplo. Analysis and interpretation of data: Castro-Vega, Calsina, Burnichon, Drossart, Martínez-Montes, Verkarre, Amar, Bertherat, Rodríguez-Antona, Favier, Robledo, and Gimenez-Roqueplo. Drafting and revising the manuscript: Castro-Vega, Calsina, Robledo, and Gimenez-Roqueplo. Acquisition of the data: Castro-Vega, Calsina, Burnichon, Drossart, Verkarre, and Amar.

DATA AVAILABILITY STATEMENT

Detailed information of the genomic platforms and cohorts analyzed was reported elsewhere (2).

Luis Jaime Castro-Vega^{1,#} 

Bruna Calsina^{2,#} 

Nelly Burnichon^{1,3}

Tom Drossart^{1,3}

Ángel M Martínez-Montes²

Virginie Verkarre^{1,4}

Laurence Amar^{1,5}

Jérôme Bertherat^{6,7}

Cristina Rodríguez-Antona^{2,8}

Judith Favier¹

Mercedes Robledo^{2,8}

Anne-Paule Gimenez-Roqueplo^{1,3,7}

¹ INSERM, PARCC, Equipe labellisée par la Ligue contre le cancer, Paris University, Paris, France

² Hereditary Endocrine Cancer Group, Human Cancer Genetics Program, Spanish National Cancer Research Centre (CNIO), Madrid, Spain

³ Genetics Department, Assistance Publique-Hôpitaux de Paris, Hôpital européen Georges Pompidou, Paris, France

⁴ Department of Pathology, Assistance Publique-Hôpitaux de Paris, Hôpital Européen Georges Pompidou, Paris, France

⁵ Hypertension unit, Assistance Publique Hôpitaux de Paris, Hôpital Européen Georges Pompidou, Paris, France

⁶ Paris University, INSERM, Institut Cochin, Paris, France

⁷ Rare Adrenal Cancer Network COMETE, Paris, France

⁸ *Centro de Investigación Biomédica en Red de Enfermedades Raras (CIBERER), Madrid, Spain*

Correspondence

Luis Jaime Castro-Vega, MD, PhD, Genetics and Metabolism of Rare Cancers, Paris-Cardiovascular Research Center, Paris, France.
Email: luis-jaime.castro-vega@inserm.fr

Present address

Luis Jaime Castro-Vega, MD, PhD, Genetics and Development of Brain Tumors, ICM - Paris Brain Institute, Paris, France.
Email: luis.castrovega@icm-institute.org

#These authors contributed equally to this work.

ORCID

Luis Jaime Castro-Vega  <https://orcid.org/0000-0002-7232-9871>

Bruna Calsina  <https://orcid.org/0000-0002-6922-9415>

REFERENCES

1. Dahia P, Clifton-Bligh R, Gimenez-Roqueplo AP, Robledo M, Jimenez C. Metastatic pheochromocytoma and paraganglioma: proceedings of the MEN2019 workshop. *Endocr Relat Cancer*. 2020;27:T41-T52.
2. Calsina B, Castro-Vega LJ, Torres-Perez R, et al. Integrative multi-omics analysis identifies a prognostic miRNA signature and a targetable miR-21-3p/TSC2/mTOR axis in metastatic pheochromocytoma/paraganglioma. *Theranostics*. 2019;9:4946-4958.
3. Meyer-Rochow GY, Jackson NE, Conaglen JV, et al. MicroRNA profiling of benign and malignant pheochromocytomas identifies novel diagnostic and therapeutic targets. *Endocr Relat Cancer*. 2010;17:835-846.
4. Patterson E, Webb R, Weisbrod A, et al. The microRNA expression changes associated with malignancy and SDHB mutation in pheochromocytoma. *Endocr Relat Cancer*. 2012;19:157-166.
5. Tsang VH, Dwight T, Benn DE, et al. Overexpression of miR-210 is associated with SDH-related pheochromocytomas, paragangliomas, and gastrointestinal stromal tumours. *Endocr Relat Cancer*. 2014;21:415-426.
6. Ruff SM, Ayabe RI, Malekzadeh P, et al. MicroRNA-210 may be a preoperative biomarker of malignant pheochromocytomas and paragangliomas. *J Surg Res*. 2019;243:1-7.
7. Liu M, Roth A, Yu M, et al. The IGF2 intronic miR-483 selectively enhances transcription from IGF2 fetal promoters and enhances tumorigenesis. *Genes Dev*. 2013;27:2543-2548.
8. Qiao Y, Ma N, Wang X, et al. MiR-483-5p controls angiogenesis in vitro and targets serum response factor. *FEBS Lett*. 2011;585:3095-100.
9. Wang H, Zhang H, Sun Q, et al. Intra-articular delivery of antago-miR-483-5p inhibits osteoarthritis by modulating Matrilin 3 and tissue inhibitor of metalloproteinase 2. *Mol Ther*. 2017;25:715-727.
10. Bertero T, Gastaldi C, Bourget-Ponzio I, et al. miR-483-3p controls proliferation in wounded epithelial cells. *FASEB J*. 2011;25:3092-105.
11. von Lersner A, Drosen L, Zijlstra A. Modulation of cell adhesion and migration through regulation of the immunoglobulin superfamily member ALCAM/CD166. *Clin Exp Metastasis*. 2019;36:87-95.
12. Song Q, Xu Y, Yang C, et al. miR-483-5p promotes invasion and metastasis of lung adenocarcinoma by targeting RhoGDI1 and ALCAM. *Cancer Res*. 2014;74:3031-3042.

SUPPORTING INFORMATION

Additional supporting information may be found online in the Supporting Information section at the end of the article.

Appendix